Bioprocess Biosyst Eng
DOI 10.1007/s00449-015-1528-y

ORIGINAL PAPER

Electrospun polylactic acid and polyvinyl alcohol fibers as efficient and stable nanomaterials for immobilization of lipases

Péter Lajos Sóti[1] · Diana Weiser[1] · Tamás Vigh[1] · Zsombor Kristóf Nagy[1] · László Poppe[1,2] · György Marosi[1]

Received: 11 June 2015 / Accepted: 19 December 2015

Abstract Electrospinning was applied to create easy-to-handle and high-surface-area membranes from continuous nanofibers of polyvinyl alcohol (PVA) or polylactic acid (PLA). Lipase PS from *Burkholderia cepacia* and Lipase B from *Candida antarctica* (CaLB) could be immobilized effectively by adsorption onto the fibrous material as well as by entrapment within the electrospun nanofibers. The biocatalytic performance of the resulting membrane biocatalysts was evaluated in the kinetic resolution of racemic 1-phenylethanol (*rac*-**1**) and 1-phenylethyl acetate (*rac*-**2**). Fine dispersion of the enzymes in the polymer matrix and large surface area of the nanofibers resulted in an enormous increase in the activity of the membrane biocatalyst compared to the non-immobilized crude powder forms of the lipases. PLA as fiber-forming polymer for lipase immobilization performed better than PVA in all aspects. Recycling studies with the various forms of electrospun membrane biocatalysts in ten cycles of the acylation and hydrolysis reactions indicated excellent stability of this forms of immobilized lipases. PLA-entrapped lipases could preserve lipase activity and enantiomer selectivity much better than the PVA-entrapped forms. The electrospun membrane forms of CaLB showed high mechanical stability in the repeated acylations and hydrolyses than commercial forms of CaLB immobilized on polyacrylamide beads (Novozyme 435 and IMMCALB-T2-150).

Keywords Biocatalysis · Electrospinning · Immobilization · Lipase · Kinetic resolution

Introduction

Elaboration of cost-efficient methods for preparation of pure enantiomers is of great importance in the production of active pharmaceutical ingredients (API) and other fine chemicals [1–3]. The importance of catalytic and particularly biocatalytic processes within these methods is growing increasingly. Enzymatic syntheses are environmentally benign because they can be performed at ambient temperature and atmospheric pressure, aqueous medium, in many cases. The natural chirality of the proteins in the enzyme-catalyzed processes allows their application to produce pure enantiomers by stereoselective methods such as kinetic resolution (KR) [4] even on industrial scale [5, 6]. However, the production of suitable forms of enzymes might be expensive; thus research activity aiming their recyclability is urgent because multi-cycle utilization of biocatalysts could drastically cut the costs.

Recovery of the native enzyme from the reaction medium (mostly aqueous) is difficult, thus various immobilization techniques have been developed [7–10]. Enzyme immobilization can be performed by physical (adsorption, entrapment) or chemical (covalent bond, chemical cross-linking) methods [11]. The chemical methods, however, require further expensive modification of the enzyme or the support and can initiate structural changes influencing the catalytic activity negatively [9, 10] or positively [12]. The

L. Poppe and G. Marosi have contributed equally to this work.

✉ Péter Lajos Sóti
psoti@mail.bme.hu

György Marosi
gmarosi@mail.bme.hu

[1] Department of Organic Chemistry and Technology, Budapest University of Technology and Economics, Budafoki út 8., 1111 Budapest, Hungary

[2] SynBiocat Ltd., Lázár deák u. 4/1, 1173 Budapest, Hungary

Published online: 02 January 2016

methods based on physical interactions are gentle, but simple adsorption allows detachment of the enzyme from the carrier in recycling and reduces the cost-effectiveness of such biocatalysts [13, 14]. Embedding of enzymes in polymeric matrix—for instance, by the sol–gel method—can enhance their thermal and mechanic stability [14, 15], but their activity is often reduced by their restricted accessibility. When the polymer-embedded enzyme system is prepared by evaporating the solvent from a common solution, emulsion or suspension [16], the heat-sensitive enzymes tolerate only extremely gentle way of solvent evaporation. Therefore, methods which do not harm the activity of enzymes, but still fix them firmly in the solid phase are needed.

Nanosized materials such as spheres, fibers and tubes are increasingly popular in enzyme immobilizations because of their high surface-to-volume ratio [17]. Although nanoparticles and nanotubes can decrease mass transfer limitations, their dispersion and recovery can be difficult. Electrospun nanofibers of infinite length have a great potential to overcome these problems and thus are promising supports for enzyme immobilization [18]. Although reduced activity was found when cellulase was embedded in electrospun PVA nanofibers and cross-linked with glutaraldehyde [19], electrospinning technology has advantages in enzyme immobilization because the removal of solvent is performed at ambient temperature and atmospheric pressure. Electrospun nanofibers show clear advantages in catalysis because the contact between the catalyst and substrate is allowed at a very high surface area [20–23]. Whereas immobilization of enzymes on/into nanofibers were reported recently, the recyclability of the electrospun membrane biocatalysts has been poorly discussed up to now. The cellulase in electrospun PVA fixed by cross-linking retained 36 % of its initial activity after six cycles of reuse [19]. Recycling test with Lipase F-AP immobilized in PVA indicated a decrease of enzyme activity below 50 % after two cycles [24]. Glucose oxidase immobilized in PLA retained only about 50 % of initial activity after three cycles [25]. These results are still not suitable for economic industrial use.

Our aim was to investigate the efficiency of immobilization methods of lipases applicable for KR in organic and aqueous media using biocompatible hydrophilic PVA and biodegradable hydrophobic PLA nanofibers, furthermore, to compare the catalytic properties of the resulting membrane biocatalysts in KR process. Although immobilization of enzymes in PVA and PLA is known, comparison of lipases immobilized in PVA and PLA nanofiber membranes and their use for KR has not yet investigated. Furthermore, our aim was to evaluate and improve the reusability of lipase biocatalyst membrane prepared this way.

Experimental

Materials

Sodium phosphate mono- and dibasic, PVA (Mowiol® 18-88), *rac*-**1**, *rac*-**2**, vinyl acetate, Novozym® 435 (N435, recombinant lipase B from *Candida antarctica* expressed in *Aspergillus niger*, adsorbed on acrylic resin) and Amano Lipase PS (lipase from *Burkholderia cepacia*) were obtained from Sigma-Aldrich (Saint Louis, MO, USA). CaLB (lipase B from *C. antarctica*, recombinant, lyophilized powder) was a product of c-LEcta Ltd (Leipzig, Germany). Chiral Vision Immobead T2-150 (CV, *C. antarctica* lipase B covalently attached to dry acrylic beads) was the product of ChiralVision BV (Leiden, Netherlands). PLA (D-isomer < 5 %, PURASORB® PL 24) was obtained from PURAC (Gorinchem, Netherlands). Solvents (*n*-hexane, methyl *tert*-butyl ether, chloroform, ethanol) from Molar Chemicals (Budapest, Hungary) were freed from water and/or freshly distilled prior to use. *N*,*N*-Dimethylformamide (DMF) was obtained from Merck (Budapest, Hungary).

Fourier transform infrared spectrometry

KBr tablets were prepared for the Fourier transform infrared (FTIR) spectrometry measurements of native or immobilized enzymes and PLA fibers. The KBr tablets were analyzed by Bruker Tensor 37-type spectrometer equipped with deuterated triglycine sulfate detector (Ettlingen, Germany) in the range of 4000–700 cm^{-1} with a resolution of 4 cm^{-1}.

Scanning electron microscopic (SEM) investigation

Morphology of the nanofiber membranes was examined by a JEOL JSM 6380LA (Tokyo, Japan) scanning electron microscope (acceleration voltage: 20–25 kV). Samples for SEM were dried under vacuum, mounted on metal stubs, and sputter-coated with gold/silver binary alloy.

Lipase entrapment by electrospinning

To the polymer solution (PVA solution: 450 mg, 10 % w/w PVA in distilled water; PLA solution: 900 mg, 5 % w/w PLA in chloroform—DMF 6:1) a freshly prepared solution of lipase in sodium phosphate buffer was added (33.5 μL, buffer: 100 mM, pH 7.5, crude lipase powder concentration: 150 mg mL^{-1}). The resulting mixture was agitated in an ultrasound bath for 25 min and then electrospun using an infusion pump (Aitecs SEP-10S Plus syringe pump, Vilnius, Lithuania; PVA solution: at

Table 1 Catalytic behavior of the electrospun nanofibrous membrane-immobilized lipases and the non-immobilized lipase powders in the KR of *rac*-**1** (reaction time: 2 h, immobilized crude enzyme powder content 10 w/w%)

Entry	Lipase	Polymer	Immobilization	c (%)	E	U_B (U g^{-1})	Y_A (%)[a]
1[b]	Lipase PS	–	–	42	>200	29[c]	100
2	Lipase PS	PLA	Adsorption	15	>200	10	356
3	Lipase PS	PVA	Entrapment	21	≫200	14	499
4[b]	Lipase PS	PLA	Entrapment	47	≫200	32	1121
5	CaLB	–	–	5	≫200	4[c]	100
6	CaLB	PLA	Adsorption	19	>200	13	3754
7	CaLB	PVA	Entrapment	22	>200	15	4574
8[b]	CaLB	PLA	Entrapment	32	≫200	22	6341

[a] The improved Y_A probably due to the decreased length of the diffusion pathway of the substrate

[b] Above 30 % conversions, the overall reaction rates were limited significantly by the decrease of substrate [(*R*)-**1**] concentration

[c] For the non-immobilized lipase powders $U_B = U_E$

0.016 mL min^{-1}; PLA solution: at 0.13 mL min^{-1}). The distance between the collector and the spinneret (ID = 0.4 mm) was 10–23 cm. Constant voltage (in the range of 10–30 kV) was applied to the spinneret using a direct current power supplier (NT-35 High Voltage DC Supply MA2000, Nagykanizsa, Hungary). Electrospun fibers were collected on alumina foil affixed to the collector. Electrospinning experiments were performed at room temperature (24 ± 2 °C). Details of the samples prepared by entrapment are given in Table 1.

Lipase adsorption on the electrospun nanofibers

First, enzyme-free PLA membrane was prepared (as described in "Lipase entrapment by electrospinning" section and [26]) and freshly prepared lipase solution in sodium phosphate buffer (1 mL, buffer: pH 7.5, 100 mM, crude lipase powder concentration: 5 mg mL^{-1}) was poured onto the enzyme-free PLA membrane (45 mg) and shaken at 4 °C for 24 h. The resulted membrane-adsorbed lipase was washed twice with 2-propanol (2 mL) and once with *n*-hexane (2 mL). Finally, the membrane was dried at room temperature for 2 h. Details of the samples prepared by adsorption technique are given in Table 1.

Kinetic resolutions of *rac*-1 and *rac*-2 with native and immobilized lipases

Immobilized (electrospun membrane or acrylic resin based bead) or native lipase (50 mg) was added to a solution of racemic 1-phenylethanol *rac*-**1** (50 µL; 50.6 mg; 0.41 mmol) in hexane/methyl *tert*-butyl ether/vinyl acetate 6/3/1 (v/v) mixture (1 mL) or to an emulsion of racemic 1-phenylethyl acetate *rac*-**2** (50 µL; 51.4 mg; 0.31 mmol) in phosphate buffer (1 mL; pH 7.5, 100 mM) in a screw capped amber glass vial. The resulting mixtures were shaken (1000 rpm) at 30 °C for 2 h. Samples (50 µL) from the reactions were diluted with ethanol (1000 µL) and analyzed by gas chromatography (GC) on an Agilent 4890 equipment using Hydrodex β-6TBDM column (Machery-Nagel, 25 m × 0.25 mm × 0.25 µm, heptakis-(2,3-di-*O*-methyl-6-*O*-*t*-butyldimethylsilyl)-β-cyclodextrin) [FID (250 °C), injector (250 °C), H_2 (12 psi, split ratio: 1:50), oven temperature: 120 °C]. GC data, t_r (min): 3.8 [(*S*)-**2**], 4.2 [(*R*)-**2**], 5.5 [(*R*)-**1**], 5.7 [(*S*)-**1**].

Conversion (c), enantiomeric excess (ee) and enantiomeric ratio (E) were determined by GC. Enantiomeric ratio (E) was calculated from c and enantiomeric excess of the product (ee_P) using the equation $E = \ln[1 - c(1 + ee_P)]/\ln[1 - c(1 - ee_P)]$ [27]. Due to its sensitivity to experimental error E values in the 100–200 range are given as >100, in the range of 200–500 as >200 and above 500 as ≫200. Effective specific activity of the biocatalyst (U_B) was determined using the equation $U_B = (n_{rac} \times c)/(t \times m_B)$ [where n_{rac} (µmol) is the amount of the racemic substrate, t (min) is the reaction time and m_B (g) is the mass of biocatalyst] [28]. Effective specific activity of the crude non-immobilized enzyme powder (U_E) was determined using the equation $U_E = (n_{rac} \times c)/(t \times m_E)$ [where n_{rac} (µmol) is the amount of the racemic substrate, t (min) is the reaction time and m_E (g) is the mass of the crude non-immobilized enzyme powder] [29]. The activity yield [Y_A (%)] can be calculated from the effective specific activity of the immobilized biocatalyst (U_B) compared to the effective specific activity of the non-immobilized enzyme (U_E) using the equation $Y_A = 100 \times U_B/U_E$ which is equal to the equation $Y_A = 100 \times [(n_{rac} \times c)/(t \times m_B)]/U_E$ [29].

Recycling of the lipase biocatalysts

Different forms of lipase biocatalysts were tested in KR of *rac*-**1** and *rac*-**2** by the same reactions which are described in "Kinetic resolutions of *rac*-**1** and *rac*-**2** with native and immobilized lipases" section. After the reaction (reaction time 2 h) the biocatalysts were filtered from the reaction mixture and washed with hexane/methyl *tert*-butyl ether

2/1 (v/v) solvent mixture (3 mL, three times) before reuse. Samples were dried to constant weight at room temperature and biocatalysts were simply introduced into a new reaction medium at the same biocatalyst and substrate concentration as in the first reaction (in this way the mass loss occurred in a cycle was taken into account).

Results and discussion

Two electrospinning-based immobilization methods (adsorption and entrapment) of two lipases (crude powder forms of Lipase PS and CaLB) with two matrix-forming polymers (polyvinyl alcohol, PVA and polylactic acid, PLA) were selected for this study. During the experiments, commercially available polymers with completely different chemical structure and physicochemical properties were used in order to investigate their effect on the immobilization. Tests with the forming nanofibrous membrane-immobilized lipases indicated that these forms were applicable as biocatalyst in KRs of 1-phenylethanol by acylation in organic media and of 1-phenylethyl acetate by hydrolysis in aqueous phosphate buffer. In addition, the composition and fiber morphology of the nanofiber membrane-based biocatalysts were also evaluated by FTIR and SEM and finally their reusability was compared to commercial biocatalysts.

Analysis of the immobilized nanofibrous and non-immobilized lipases by FTIR spectrometry

The electrospun fiber-entrapped lipases, prepared as described in "Lipase entrapment by electrospinning" section, were analyzed by FTIR spectrometry in order to verify the presence and interactions of enzymes in the PLA fibers. The results are shown in Fig. 1.

The bands for stretching vibration of C=O part of peptide bonds are the most characteristic to the enzymes. Regarding the CaLB and Lipase PS, the peptide bond C=O bands appeared at 1645, and 1652 cm^{-1} respectively. The intensive band of PLA nanofiber systems at 1759 cm^{-1} is characteristic to the ester C=O bond in PLA [30]. The characteristic IR bands of enzymes embedded in PLA appeared slightly up-shifted compared to their original value, suggesting interaction between the enzymes and PLA (for CaLB in PLA fiber: 1681 cm^{-1}, from 1645 cm^{-1}; for Lipase PS in PLA fiber: 1682 cm^{-1} from 1652 cm^{-1}). When the lipases were adsorbed on electrospun nanofibers (not shown), no significant changes were found in their spectra.

The CaLB-containing electrospun PLA membranes were also analyzed after the recycling tests. Figure 1e shows the characteristic FTIR band associated with

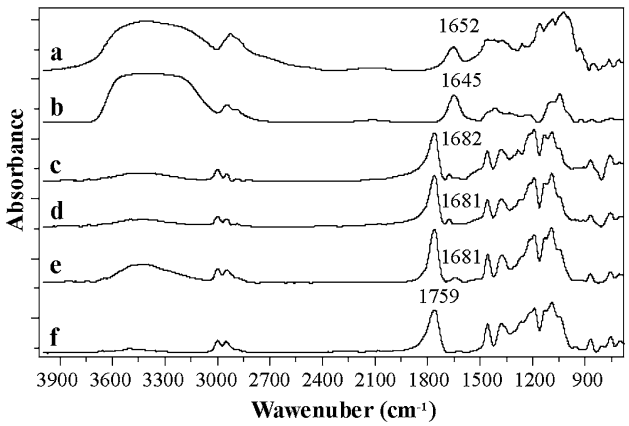

Fig. 1 FTIR spectra of Lipase PS (*a*), CaLB (*b*), Lipase PS entrapped into PLA (*c*), CaLB entrapped into PLA (*d*), CaLB entrapped in PLA after ten reusing (*e*) and PLA fibers without lipase (*f*)

vibration of peptide bonds at about 1681 cm^{-1}—which is the same found for the fresh biocatalyst (Fig. 1d)—confirming that leaching of the immobilized enzymes can be avoided by entrapment.

Morphology and structure of electrospun nanofiber lipase biocatalyst systems

Scanning electron microscopy was used to investigate the structure of lipase-containing systems to correlate their morphology with their catalytic properties. SEM images of the various lipase preparations are shown in Figs. 2 and 6.

Images of the native Lipase PS (Fig. 2a) and electrospun PLA fibrous membrane without enzyme (Fig. 2b) indicated large aggregates of the Lipase PS (diameter >10 μm) and nanofibrous systems of large surface area ($\sim$40,000 $cm^2\ g^{-1}$ in case of PLA with density of 1.25 g cm^{-3} for fiber of infinite length with average diameter of 800 nm). Fine dispersion of Lipase PS within or onto the electrospun fiber-based systems (Fig. 2c, d, respectively) can dramatically increase the availability of the lipase molecules resulting in an apparent increase of the activity of the nanofibrous membrane immobilized biocatalysts (U_B) compared to the original activity of the Lipase PS powder (U_E).

The final forms of the immobilized Lipase PS, manufactured either by adsorption or by encapsulation techniques, are fibrous web with easily available large surface (Fig. 2c, d). SEM investigations indicated that the aggregate size of the original Lipase PS preparation (up to 100 μm, Fig. 2a) reduced remarkably after the adsorption of the lipase from an aqueous solution (Fig. 2c). In the case of the lipase entrapment—by adding the enzyme buffer to the polymer solution before the formation of electrospun fibers—no significant the increase of fiber thickness was observed (Fig. 2d) compared to the lipase-free fibers (Fig. 2b).

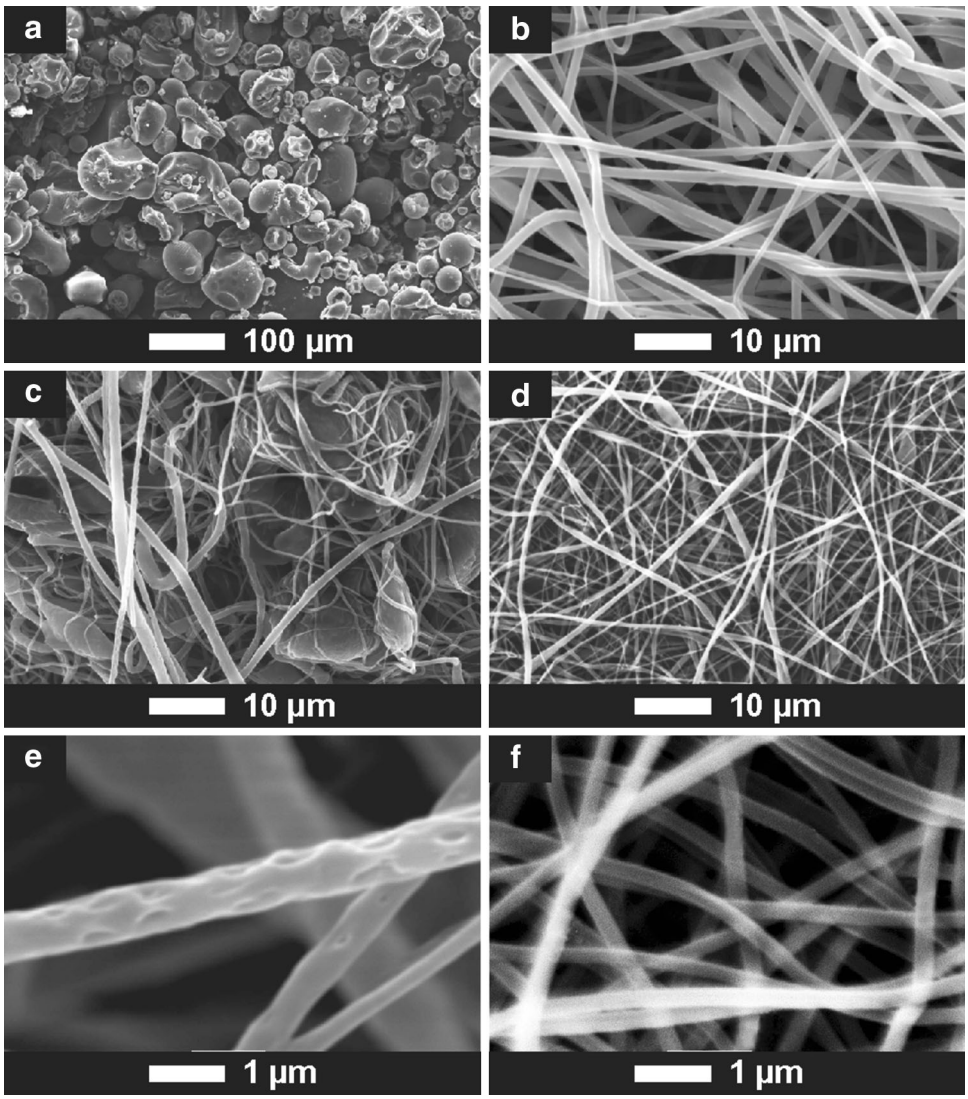

Fig. 2 SEM images of non-immobilized Lipase PS enzyme powder (**a**). PLA nanofibers without enzyme (**b**). Lipase PS adsorbed on PLA nanofibers (**c**). Lipase PS entrapped in PLA nanofibers (**d**). Lipase PS in PLA nanofibers (higher magnification) (**e**). Lipase PS in PVA nanofibers (**f**)

PLA and PVA fibers with entrapped Lipase PS were compared using SEM method at larger, 20,000× magnification as well (Fig. 2e, f). It is visible that the Lipase PS-containing PLA fibers have larger average diameters (500–800 nm, Fig. 2e) than their PVA-based counterparts (200–300 nm, Fig. 2f). Another significant difference between these fibers is their surface appearance. It can be important that the characteristic roughness of the surface of PLA–enzyme fibers (Fig. 2e) increases their surface area.

Comparison of the catalytic behavior of lipases immobilized by adsorption and entrapment

The catalytic performance of the nanofibrous membrane-like immobilized lipase biocatalysts was tested in a KR process using the acylation reaction of 1-phenylethanol *rac*-**1** with vinyl acetate (Fig. 3). (*R*)- or (*S*)-enantiomers of

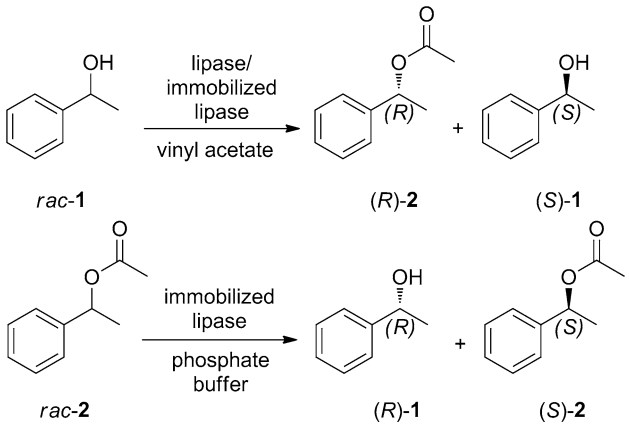

Fig. 3 KRs of racemic 1-phenylethanol (*rac*-**1**) by acylation and 1-phenylethyl acetate (*rac*-**2**) by hydrolysis for characterization of the catalytic properties of the immobilized and non-immobilized forms of lipases

1-phenylethanol are compounds with a number of potential applications. They can be building blocks for the synthesis of bioactive compounds, such as various natural products, agrochemicals and pharmaceuticals [31].

The catalytic behavior of the lipases immobilized by the various techniques were characterized by the conversion (c), enantiomeric ratio (E), apparent specific enzyme activity (U_B) and immobilization yield (Y_A) after 2 h reaction time, with fixed amounts of biocatalysts in the KR process of *rac*-**1** (Fig. 3, Table 1).

The *O*-acylated product (*R*)-**2** was formed in various conversions (c) at high enantiomeric ratio (E) in all cases (Table 1). Although Lipase PS in its PLA-entrapped form contained ten times less enzyme than the non-immobilized Lipase PS form, the highest conversion ($c = 47$ %) was achieved with the less enzyme-containing PLA-entrapped Lipase PS preparation. Although higher catalytic activity could be expected by adsorptive immobilization in contrast to entrapped counterpart due to the less restricted diffusion of substrate, the conversion in the KR process of *rac*-**1** with the entrapped lipases was always superior to that found with their adsorbed counterparts.

Comparison of the apparent specific enzyme activities of the immobilized lipases (U_B) with the same characteristic of the non-immobilized lipase powders (U_E), shown in Table 1, provides further understanding. Although the apparent specific activities of CaLB preparations (U_B = 4–22 U g^{-1}) are in the same order of magnitude as of the corresponding Lipase PS biocatalysts (U_B = 10–32 U g^{-1}), the activity yield (Y_A) enhancement achieved by nanofibrous immobilization compared to the original powder form for CaLB (Y_A = 3754–6341 %) is almost one magnitude of order higher than for Lipase PS (Y_A = 499–1121 %). In general, all the nanofibrous lipase immobilizations resulted in a huge enhancement in alcohol acylation activity in organic medium compared to the non-immobilized forms. Considering the insolubility of crude enzyme powder in the organic medium, this activity enhancement can be interpreted by the fact that the non-immobilized lipase powders remained as aggregates in the organic liquid causing significant diffusional limitations (the enzyme molecules inside the aggregates are much less available for the substrate and release of the product is also hindered). In contrast, the membrane-immobilized lipase preparations are more dispersed in a nanofibrous system having large surface area (Fig. 2e) and thus diffusional limitations are much less pronounced. The decreased length of the diffusion pathway of the substrate to the active sites can explain the enormous enhancement of the apparent activity achieved with the immobilized nanofibrous enzyme systems.

For the indirect evidence of enzyme dispersion into the fibers, dynamic light scattering (DLS; Nanotrac NPA-250, Microtrac Co., USA) measurement was used determining the dispersion of enzymes in the polymer solution before the electrospinning. In case of PVA–enzyme solution, the DLS data confirmed less than 50 nm particle sizes. Considering the rapid solvent evaporation at fiber formation, the time for enzyme aggregation is very limited leading to high dispersity of enzymes in the matrices.

Although the enzymes entrapped within a polymer matrix are generally assumed to be less available, the entrapped lipases in our systems outperformed the corresponding adsorbed form of the same lipase. The slightly less significant activity enhancement of the adsorbed lipases compared to their entrapped counterparts, found in this study, can be rationalized by some aggregation within the adsorbed enzyme layer (Fig. 2c). Therefore it can be supposed that the activity enhancement caused by the increased surface area of immobilized nanofibrous forms, depends on the actual case and applied technique.

The degree of enantiomer selectivity is another crucial issue in KR. Therefore, the enantiomeric ratio (E) which is the most appropriate measure of the enantiomer selectivity of a reaction was also determined for the KR process with *rac*-**1** for the native and for the membrane immobilized lipases (Table 1). The originally high enantiomer selectivity of non-immobilized CaLB ($E \gg 200$) decreased slightly by adsorption ($E > 200$), while the entrapped CaLB maintained its high $E \gg 200$ value. In the case of Lipase PS, the E values of both the native and adsorbed enzymes fall in the range of 200–500 ($E > 200$), while E of the entrapped Lipase PS exceeded 500 ($E \gg 200$) indicating that entrapment can increase the enantiomer selectivity. Similar increase achieved by immobilization in solid support was reported by Queiroz et al. [32].

Because the entrapped forms of the lipases proved to be superior to the adsorbed forms in all aspects, only the membrane-entrapped lipases were investigated in the further experiments.

Comparison of lipase encapsulation within PVA and PLA electrospun nanofibers

Influence of polymer type on the catalytic performance of the nanofiber-entrapped lipases was also apparent. In addition to their morphology (see "Morphology and structure of electrospun nanofiber lipase biocatalyst systems" section), further properties of the two polymeric types differ significantly because PVA is water soluble and flexible, whereas PLA is water insoluble and rigid polymer. During PVA-entrapment, the aqueous enzyme solution was mixed with an aqueous polymer solution, while during the PLA-entrapment, a chloroform solution of the polymer was emulsified with the aqueous enzyme. Consequently, the PVA-based biocatalysts can be applied

only in non-protic organic media whereas the high molecular weight PLA-based forms are applicable both in aqueous and in most organic media. Performance of the resulting electrospun-nanofibrous-membrane-entrapped lipases in PVA and PLA can be compared based on the results given in Table 1.

Data in Table 1 indicate that the lipases entrapped nanofibers surpass the activity of the corresponding non-immobilized lipase powder. The fact that PLA-entrapped lipases (entries 4 and 8) exhibited significantly higher conversion after 2 h in the KR of *rac*-**1** than that of their PVA-based counterparts (entries 3 and 7, respectively) was surprising because PLA fibers were thicker than PVA fibers (Fig. 2e, f). Moreover, in spite of the fact that the chloroform–DMF 6:1 mixture (used for preparation PLA-enzyme systems according to "Lipase entrapment by electrospinning" section) could harm the catalytic activity of enzymes the PLA fibers formed with these solvents ensured more active form of the lipases than PVA. These results can be explained by the higher hydrophobicity of the PLA matrix compared to that of PVA, which can better stabilize the active, open conformation of the lipases. This is also supported by the fact that the more affected Lipase PS contains flexible, large active-site-covering lid, which is much smaller and less mobile in the case of CaLB. In addition, PLA fibers have porous structure which increase the surface area of the fibers and facilitate the contact between the enzyme and the substrate in solution, while the surface of PVA fibers is uniformly continuous and smooth.

The enantiomer selectivity in the KR of *rac*-**1** was excellent for both the PLA- and the PVA-entrapped forms of Lipase PS and CaLB ($E > 200$). According to the previous results, a high degree of enantiomeric ratio ($E > 100$) enables the preparation of both enantiomeric forms [i.e. (*R*)-**2** and (*S*)-**1**] in appropriate enantiomeric purity (ee > 95 %) and productivity (yield > 45 %, based on the racemic substrate) [33].

Recycling study of immobilized biocatalysts

Recyclability of the electrospun nanofiber-based immobilized CaLB and Lipase PS biocatalysts was investigated in the subsequent tests (Fig. 4). In all cases, the apparent specific biocatalytic activity or conversion (U_B or c) of the nanofiber-entrapped forms of both lipases in the second round were considered as 100 % for the subsequent rounds because the biocatalysts showed the highest activity after the first reaction (Fig. 4a, c).

Although the non-immobilized crude enzyme powder can be recycled, owing to its insolubility in organic media, the recovery efficiency of these aggregates of irregular shape and particle size is not appropriate. The crude enzyme powder could be reused in case of Lipase PS maximum eight times and in case of CaLB only five times

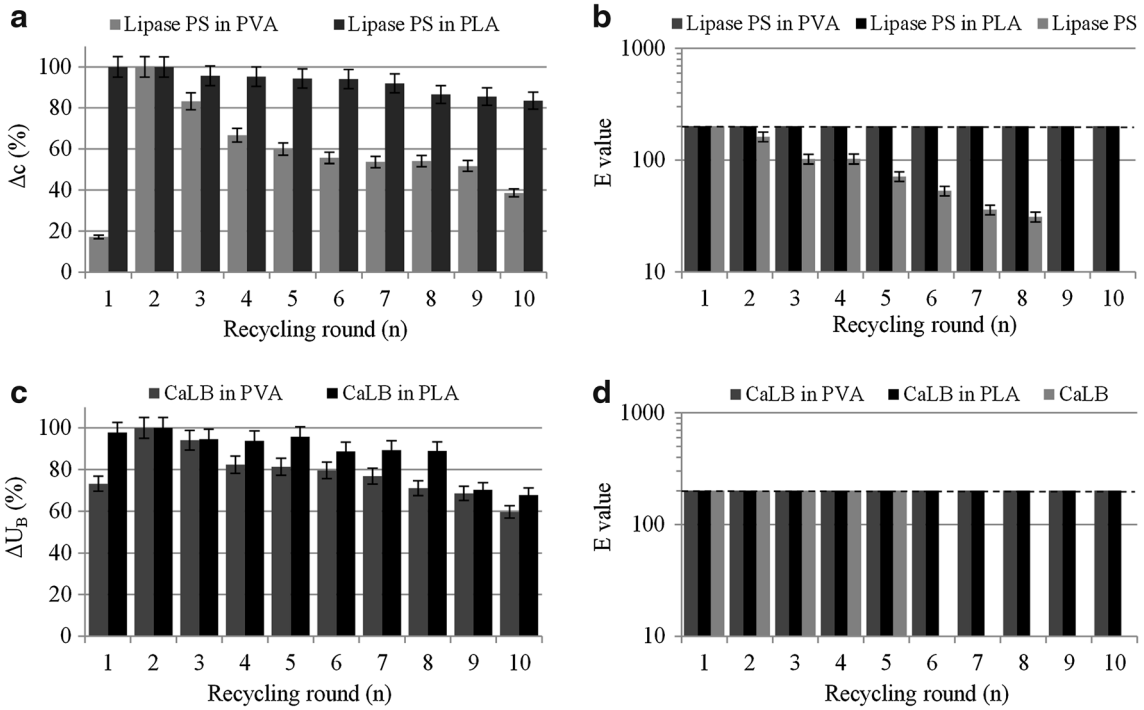

Fig. 4 Recycling of immobilized Lipase PS (**a**, **b**) and CaLB (**c**, **d**) in KRs of *rac*-**1** (ten cycles; 2 h/cycle reaction time). The *error bars* indicate ± SD ($n = 3$)

with significant loss of mass in each cycles. In contrast, the enzymes immobilized in non-woven webs were easy to recover with no detectable loss of weight and limitation in number of cycles. These showed high catalytic activities even in the 10th recycling round (see Fig. 4). CaLB entrapped in PVA or PLA preserved about 80 % of its initial activity even 6–8 cycles (Fig. 4c) and about 60 % up to cycle 10, while the entrapped Lipase PS showed 39 and 84 % residual activities. In term of recycling, the best biocatalyst seems to be the Lipase PS entrapped in PLA fibers, which kept more than 80 % of its original conversion up to ten cycles.

The enantiomer selectivity was also investigated during the repetitive uses. The different forms of CaLB biocatalysts catalyzed the reactions with excellent enantiomer selectivity and no significant changes were observed during the recycling ($E \gg 200$; Fig. 4d). In case of Lipase PS, the non-immobilized form showed rapid decrease of E after the 1st reaction (it is noted the conversions of substrate were above 30 % in all eight recycling round). In contrast, the both entrapped forms preserved the high E value ($E \gg 200$) in all recycling rounds (Fig. 4b) indicating the differences between native and entrapped enzymes. This beneficial preservation of selectivity is due probably to the hindered mobility of the entrapped lipase molecules in the polymer matrices, which protects the initial open conformation of lipase, promoting unmodulated enantiomer preference [12].

On the basis of the recycling studies with the nanofiber-entrapped lipases, one can conclude that the outstanding performance of the lipases in PLA can be explained by its good biocompatibility. This is probably in connection with the shift of peptide band observed in the relevant FTIR spectrum (Fig. 1) suggesting secondary bonds between the polymeric matrix and the enzyme, which can contribute to the efficiency. Decrease of activity in the course of recycling can happen due to two reasons: (1) the enzyme molecules can be leached from the polymer fibers, (2) denaturation (i.e. change of the active conformation) of the enzymes. It seems that PLA as fiber-forming polymer can stabilize the lipases better than PVA in both of these aspects.

Finally, recycling of CaLB entrapped in PLA was compared to that of two relevant commercial immobilized forms of CaLB namely N435 and CV. The KR of *rac*-**1** was repeated to observe the reproducibility of entrapped CaLB and the experiments were extended to KR of 1-phenylethyl acetate *rac*-**2** by enantioselective hydrolysis (Fig. 3).

Due to the high degree of enantiomer selectivity and high initial activity of the acryl resin based CaLB N435, conversion of racemic 1-phenylethanol *rac*-**1** in the first reaction by acylation in organic media stopped at the maximal 50 % after consumption of all the (*R*)-**1**, thus the specific activity of the biocatalyst could not be estimated (Table 2). Use of second-batch electrospun PLA-CaLB web led to 32 % conversions in the KR of *rac*-**1** (Table 2, entry 3), same as for the first-batch electrospun PLA-CaLB web (Table 1, entry 8) indicating the reproducibility of the immobilization method. The use of acryl resin attached CV form resulted in 34 % conversion which is comparable to the catalytic performance of electrospun PLA membrane-entrapped CaLB.

With all the three CaLB forms the enantiomeric ratio in the KRs of *rac*-**1** were excellent ($E \gg 200$).

Table 2 shows that the hydrolysis of racemic 1-phenylethyl acetate (*rac*-**2**) in aqueous media took place with all the three forms of CaLB resulting in high conversions (50, 50 and 41 %) after 2 h reaction time. In the hydrolytic reaction commercial immobilized CaLBs showed high selectivity and activity ($E > 200$ and $c = 50$ %), which slightly lower (but still acceptable) when the PLA-entrapped CaLB biocatalysts ($E > 100$ and $c = 41$ %) was used [33]. It should be noted that similar selectivity ($E > 100$) was determined in case of non-immobilized CaLB form.

Recycling of the three immobilized forms of CaLB revealed some differences. The PLA-entrapped form of CaLB exhibited significantly higher stability under the investigated conditions than the acryl resin based N435 or CV forms. The PLA membrane biocatalyst preserved its catalytic properties invariably in both types of KRs (Fig. 5) while the acrylic polymer based CaLBs could only be recycled up to two–four cycles due to extensive mass loss caused by mechanical fragmentation as confirmed by SEM investigations (Fig. 6). The PLA-entrapped CaLB preserved its initial fibrous structure (Fig. 6a) after several

Table 2 Catalytic behavior of the PLA-membrane-immobilized CaLB and two commercial immobilized CaLBs in the KR of *rac*-**1** and *rac*-**2** (reaction time: 2 h)

Entry	Biocatalyst	Immobilization	KR of *rac*-**1**		KR of *rac*-**2**	
			c (%)	*E*	*c* (%)	*E*
1	N435	Adsorption	50	≫200	50	>200
2	CV	Covalent	34	≫200	50	>200
3	CaLB in PLA	Entrapment	32	≫200	41	>100

Above 40 % conversion, the overall reaction rate was seriously limited by decrease of substrate concentration

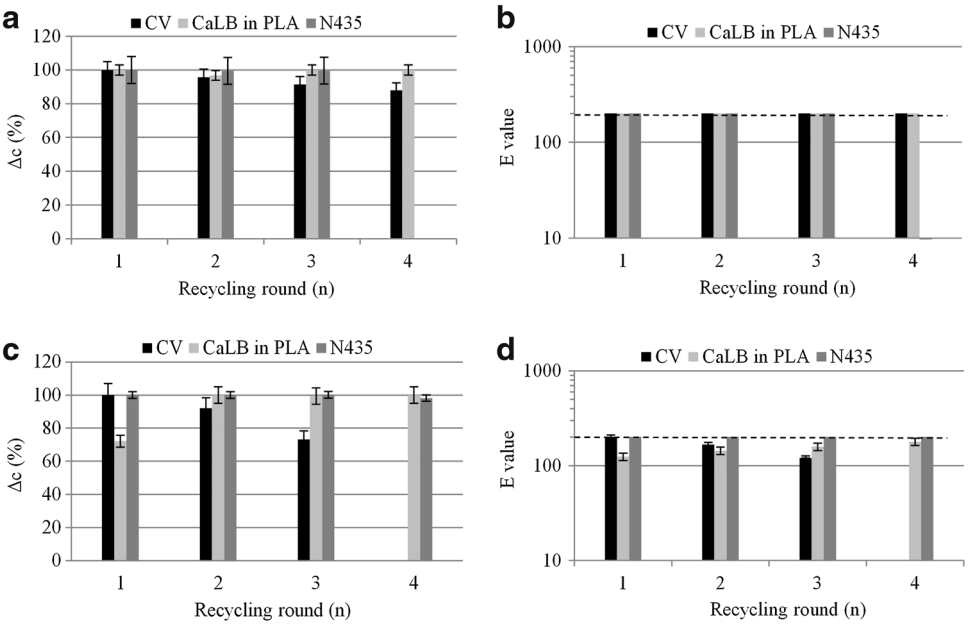

Fig. 5 Changes of conversion and enantiomer selectivity of immobilized CaLB biocatalysts in repeated KRs of *rac*-**1** by acylation in organic media (**a**, **b**) and *rac*-**2** by hydrolysis in aqueous media (**c**, **d**). The *error bars* indicate ± SD ($n = 3$)

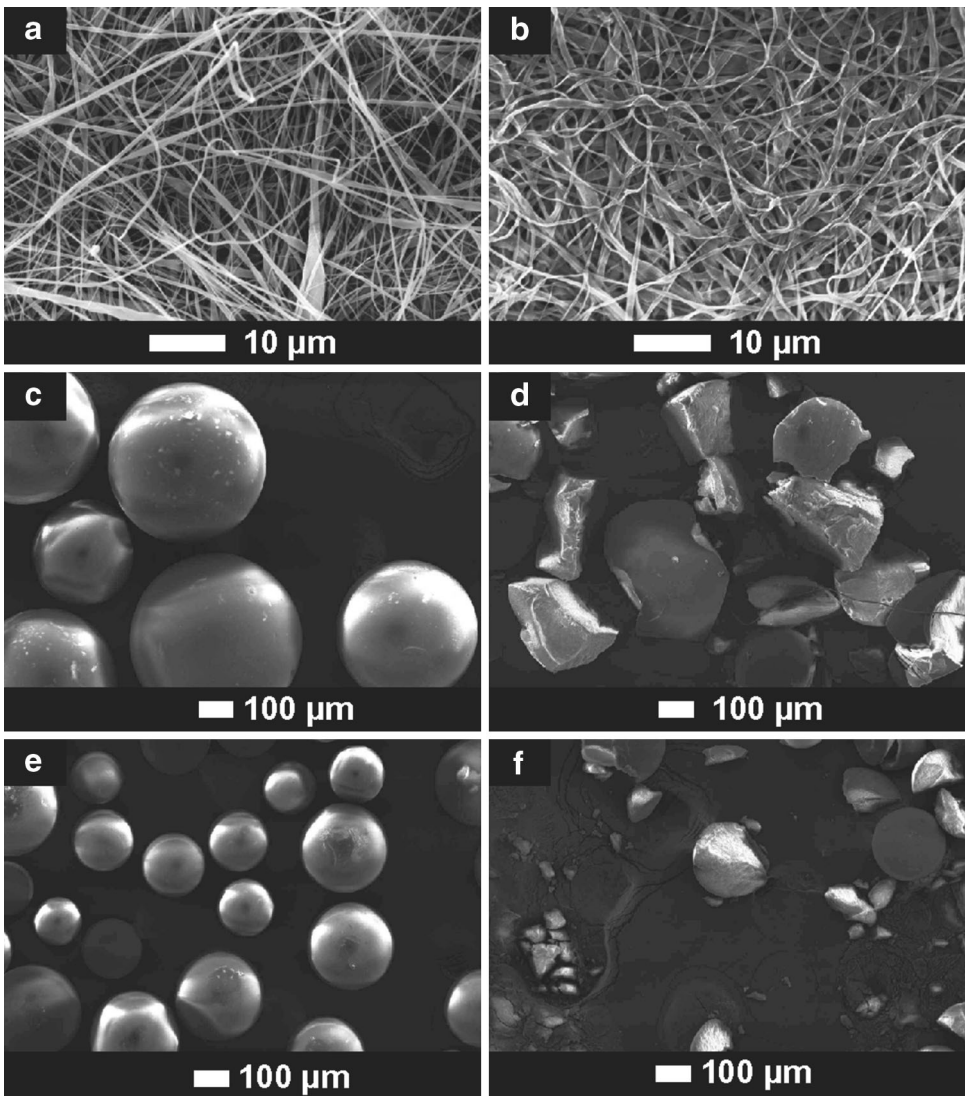

Fig. 6 SEM images of different forms of the immobilized CaLB before (*left column*) and after (*right column*) use in four cycles. CaLB entrapped in PLA nanofiber (**a**, **b**); CaLB N435 form (**c**, **d**) and CaLB CV form (**e**, **f**)

runs (Fig. 6b) while the acrylic polymer beads were fragmented after 4 cycles (Fig. 6d, f). The severe mass loss of fragmented beads allowed the recycling of N435 and CV forms of CaLB only for 4 cycles. Activity and selectivity data presented in Fig. 5 for the PLA-entrapped CaLB in both media compared to the relevant data of the acryl resin based CaLBs indicate the enhanced preservation of stability of CaLB entrapped within the electrospun PLA fibers.

Conclusion

Various types of selective biotransformations, such as KR of 1-phenylethanol *rac*-**1** in organic media and 1-phenylethyl acetate *rac*-**2,** could be performed with high efficiency in aqueous system using lipases (Lipase PS and CaLB) immobilized in polymer nanofibers. The hydrophilic (PVA) matrix-forming polymer is applicable only in organic media while the hydrophobic (PLA) could be applied in both organic and aqueous systems. The experiments confirmed that lipases preserved their enzymatic activity during and after fiber formation in electrostatic field of high voltage. Activity of the investigated membrane-immobilized lipases improved significantly compared to the non-immobilized powder forms due to the large surface area of the nanofibrous membrane system and high degree of dispersion of the lipases. Furthermore, this study indicated for the first time that PLA-based lipase-entrapment is especially suitable to form membrane biocatalysts of high activity, selectivity and excellent stability for synthetic applications such as KR. The nanofibrous entrapped lipase biocatalysts preserved most of their biocatalytic activity (>80 %) even after ten times of recycling. This methodology for enzymatic reaction is simple, effective, easy to use, and can be performed under environmentally friendly conditions.

The applied polymer matrices are biodegradable; thus their waste, after several cycles of use, degrades biologically without polluting the environment. A special advantage of PLA matrix is its insolubility and stability in most of the common solvents, including water, rendering its use feasible in various types of reaction. In addition, the PLA-entrapped CaLB had much better mechanical stability than the commercial acrylic polymer bead-based CaLBs due to negligible fragmentation and mass loss of biocatalysts upon recycling from both organic and aqueous reaction systems.

The continuous process of electrospinning produces endless nanostructured fibers that can be used to form non-woven membranes of high porosity. Because the non-woven membrane structure of the electrospun biocatalysts enables construction of biocatalytic membrane reactors for KR even at industrial scale.

Acknowledgments The research was supported by the OTKA Research Fund (code 112644 and code 108975). Besides this project is supported by the New Széchenyi Plan (Project ID: TÁMOP-4.2.1/B-09/1/KMR-2010-0002), János Bolyai Research Scholarship of the Hungarian Academy of Sciences and MedInProt Project. The authors would like to express their special thanks to NanGenex Inc., (Budapest, Hungary) for DLS measurements.

References

1. Zarie ES, Kaidas V, Gedamu D, Mishra YK, Adelung R, Furkert FH, Scherließ R, Steckel H, Groessner-Schreiber B (2012) Solvent free fabrication of micro and nanostructured drug coatings by thermal evaporation for controlled release and increased effects. PLoS One. doi:10.1371/journal.pone.0040746
2. Breuer M, Ditrich K, Habicher T, Hauer B, Kesseler M, Stürmer R, Zelinski T (2004) Industrial methods for the production of optically active intermediates. Angew Chem Int Ed 43:788–824. doi:10.1002/anie.200300599
3. Dlugy C, Wolfson A (2007) Lipase catalyse glycerolysis for kinetic resolution of racemates. Bioprocess Biosyst Eng 30:327–330. doi:10.1007/s00449-007-0128-x
4. Ghanem A, Aboul-Enein HY (2004) Lipase-mediated chiral resolution of racemates in organic solvents. Tetrahedron Asymmetr 15:3331–3351. doi: 10.1016/j.tetasy.2004.09.019
5. Kapoor M, Gupta MN (2012) Lipase promiscuity and its biochemical applications. Process Biochem 47:555–569. doi:10.1016/j.procbio.2012.01.011
6. Liese A, Seelbach K, Wandrey C (2006) Industrial biotransformations. WILEY-VCH Verlag GmbH & Co. KGaA, Weinheim
7. Sheldon RA (2007) Enzyme Immobilization: the quest for optimum performance. Adv Synth Catal 349:1289–1307. doi:10.1002/adsc.200700082
8. Rodrigues RC, Ortiz C, Berenguer-Murcia Á, Torres R, Fernández-Lafuente R (2013) Modifying enzyme activity and selectivity by immobilization. Chem Soc Rev 42:6290–6307. doi:10.1039/c2cs35231a
9. Brady D, Jordaan J (2009) Advances in enzyme immobilisation. Biotechnol Lett 31:1639–1650. doi:10.1007/s10529-009-0076-4
10. Dyal A, Loos K, Noto M, Chang SW, Spagnoli C, Shafi KVPM, Ulman A, Cowman M, Gross RA (2003) Activity of *Candida rugosa* lipase immobilized on gamma-Fe_2O_3 magnetic nanoparticles. J Am Chem Soc 125:1684–1685. doi:10.1021/ja021223n
11. Garcia-Galan C, Berenguer-Murcia Á, Fernandez-Lafuente R, Rodrigues RC (2011) Potential of different enzyme immobilization strategies to improve enzyme performance. Adv Synth Catal 353:2885–2904. doi:10.1002/adsc.201100534
12. Mateo C, Palomo JM, Fernandez-Lorente G, Guisan JM, Fernandez-Lafuente R (2007) Improvement of enzyme activity, stability and selectivity via immobilization techniques. Enzyme Microb Technol 40:1451–1463. doi:10.1016/j.enzmictec.2007.01.018
13. Lei J, Fan J, Yu C, Zhang L, Jiang S, Tu B, Zhao D (2004) Immobilization of enzymes in mesoporous materials: controlling the entrance to nanospace. Microporous Mesoporous Mater 73:121–128. doi:10.1016/j.micromeso.2004.05.004
14. Avnir D, Coradin T, Lev O, Livage J (2006) Recent bio-applications of sol–gel materials. J Mater Chem 16:1013–1030. doi:10.1039/b512706h

15. Weiser D, Boros Z, Hornyánszky G, Tóth A, Poppe L (2012) Disubstituted dialkoxysilane precursors in binary and ternary sol–gel systems for lipase immobilization. Process Biochem 47:428–434. doi:10.1016/j.procbio.2011.11.023
16. Lalonde J, Margolin A (2008) Immobilization of enzymes. In: Drauz K, Waldmann H (eds) Enzym. catal. org. synth. Wiley-VCH Verlag GmbH, Weinheim, pp 163–184
17. Lee S-M, Jin LH, Kim JH, Han SO, Bin NaH, Hyeon T, Koo Y-M, Kim J, Lee J-H (2010) Beta-glucosidase coating on polymer nanofibers for improved cellulosic ethanol production. Bioprocess Biosyst Eng 33:141–147. doi:10.1007/s00449-009-0386-x
18. Ansari SA, Husain Q (2012) Potential applications of enzymes immobilized on/in nano materials: a review. Biotechnol Adv 30:512–523. doi:10.1016/j.biotechadv.2011.09.005
19. Wu L, Yuan X, Sheng J (2005) Immobilization of cellulase in nanofibrous PVA membranes by electrospinning. J Membr Sci 250:167–173. doi:10.1016/j.memsci.2004.10.024
20. Sóti PL, Telkes L, Rapi Z, Tóth A, Vigh T, Nagy ZK, Bakó P, Marosi G (2014) Synthesis of an aza chiral crown ether grafted to nanofibrous silica support and application in asymmetric Michael addition. J Inorg Organomet Polym Mater 24:713–721. doi:10.1007/s10904-014-0037-9
21. Sakai S, Liu Y, Yamaguchi T, Watanabe R, Kawabe M, Kawakami K (2010) Production of butyl-biodiesel using lipase physically-adsorbed onto electrospun polyacrylonitrile fibers. Bioresour Technol 101:7344–7349. doi:10.1016/j.biortech.2010.04.036
22. Huang X-J, Chen P-C, Huang F, Ou Y, Chen M-R, Xu Z-K (2011) Immobilization of *Candida rugosa* lipase on electrospun cellulose nanofiber membrane. J Mol Catal B Enzym 70:95–100. doi:10.1016/j.molcatb.2011.02.010
23. Nakane K, Ogihara T, Ogata N, Yamaguchi S (2005) Formation of lipase-immobilized poly(vinyl alcohol) nanofiber and its application to flavor ester synthesis. Sen'i Gakkaishi 61:313–316. doi:10.2115/fiber.61.313
24. Sakai S, Antoku K, Yamaguchi T, Kawakami K (2008) Development of electrospun poly(vinyl alcohol) fibers immobilizing lipase highly activated by alkyl-silicate for flow-through reactors. J Membr Sci 325:454–459. doi:10.1016/j.memsci.2008.08.008
25. Zhou Y, Lim L-T (2009) Activation of lactoperoxidase system in milk by glucose oxidase immobilized in electrospun polylactide microfibers. J Food Sci 74:170–176. doi:10.1111/j.1750-3841.2009.01071.x
26. Sóti PL, Nagy ZK, Serneels G, Vajna B, Farkas A, Van der Gucht F, Fekete P, Vigh T, Wagner I, Balogh A, Pataki H, Mező G, Marosi G (2015) Preparation and comparison of spray dried and electrospun bioresorbable drug delivery systems. Eur Polym J 68:671–679. doi:10.1016/j.eurpolymj.2015.03.035
27. Chen CS, Fujimoto Y, Girdaukas G, Sih CJ (1982) Quantitative analyses of biochemical kinetic resolutions of enantiomers. J Am Chem Soc 104:7294–7299. doi:10.1021/ja00389a064
28. Tomin A, Hornyánszky G, Kupai K, Dorkó Z, Ürge L, Darvas F, Poppe L (2010) Lipase-catalyzed kinetic resolution of 2-methylene-substituted cycloalkanols in batch and continuous-flow modes. Process Biochem 45:859–865. doi:10.1016/j.procbio.2010.02.006
29. Tomin A, Weiser D, Hellner G, Bata Z, Corici L, Péter F, Koczka B, Poppe L (2011) Fine-tuning the second generation sol–gel lipase immobilization with ternary alkoxysilane precursor systems. Process Biochem 46:52–58. doi:10.1016/j.procbio.2010.07.021
30. Kister G, Cassanas G, Vert M (1998) Effects of morphology, conformation and configuration on the IR and Raman spectra of various poly(lactic acid)s. Polymer 39:267–273. doi:10.1016/S0032-3861(97)00229-2
31. Kurbanoglu EB, Zilbeyaz K, Kurbanoglu NI, Ozdal M, Taskin M, Algur OF (2010) Continuous production of (*S*)-1-phenylethanol by immobilized cells of *Rhodotorula glutinis* with a specially designed process. Tetrahedron Asymmetr 21:461–464. doi:10.1016/j.tetasy.2010.01.019
32. Queiroz N, Nascimento MG (2002) *Pseudomonas* sp. lipase immobilized in polymers versus the use of free enzyme in the resolution of (*R*, *S*)-methyl mandelate. Tetrahedron Lett 43:5225–5227. doi:10.1016/S0040-4039(02)01057-2
33. Högberg H-E (2008) Exploiting enantioselectivity of hydrolases in organic solvents organic. Synthesis with enzymes in non-aqueous media. Wiley-VCH Verlag GmbH & Co. KGaA, Weinheim